

# AgRISTARS

NAS 9-1468  
81-10132  
CR 160881

"Made available under NASA sponsorship in the interest of early and wide dissemination of Earth Resources Survey Program information and without liability for any use made thereof."

A Joint Program for  
Agriculture and  
Resources Inventory  
Surveys Through  
Aerospace  
Remote Sensing

AUGUST 5, 1980

## Supporting Research

REPORT

NUMERICAL TRIALS OF HISSE

BY: CHARLES PETERS AND FRANK KAMPE



NASA



1. Report No.	2. Government Accession No.	3. Recipient's Catalog No.
4. Title and Subtitle Numerical Trials of HISSE		5. Report Date 5 August, 1980
		6. Performing Organization Code SR-HO-00477
7. Author(s) Charles Peters and Frank Kampe		8. Performing Organization Report No. 75
9. Performing Organization Name and Address University of Houston Department of Mathematics Houston, TX 77004		10. Work Unit No.
		11. Contract or Grant No. NAS9-14689
12. Sponsoring Agency Name and Address National Aeronautics and Space Administration Lyndon B. Johnson Space Center Houston, TX 77058 Task Monitor: Dale Browne		13. Type of Report and Period Covered Technical Report
		14. Sponsoring Agency Code

15. Supplementary Notes

16. Abstract

This paper addresses the mathematical description and implementation of the statistical estimation procedure known as the Houston Integrated Spatial/Spectral Estimator (HISSE). HISSE is based on a normal mixture model and is designed to take advantage of spectral and spatial information of LANDSAT data pixels, utilizing the initial classification and clustering information provided by the AMOEBA algorithm. HISSE calculates parametric estimates of class proportions which reduce the error inherent in estimates derived from typical "classify and count" procedures common to non-parametric clustering algorithms. HISSE also singles out spatial groupings of pixels which are most suitable for labeling classes. These calculations are designed to aid the analyst/interpreter in labeling patches with a crop class label. Finally, we report HISSE's initial performance on an actual LANDSAT agricultural ground truth data set.

17. Key Words (Suggested by Author(s))

acreage estimation  
mixture density estimation  
spatial/spectral clustering

18. Distribution Statement

19. Security Classif. (of this report)

20. Security Classif. (of this page)

21. No. of Pages

22. Price\*

\*For sale by the National Technical Information Service, Springfield, Virginia 22161

TECHNICAL REPORT

NUMERICAL TRIALS OF HISSE

BY

Charles Peters and Frank Kampe

This report describes research in acreage estimation performed for the Supporting Research Project.

University of Houston  
Department of Mathematics  
Houston, TX 77004

August 5, 1980

# Numerical Trials of HISSE

by

Charles Peters and Frank Kampe

## 1. Introduction.

The Houston Integrated Spatial/Spectral Estimator (HISSE) is a statistical estimation procedure based on a normal mixture model which is designed to take advantage of spatial associations of LANDSAT data pixels produced by an automated spatial/spectral clustering algorithm. The clustering algorithm used in this experiment is the AMOEBA algorithm developed at Texas A & M University, which is based on the three assumptions listed below [1]. AMOEBA detects spatially connected sets of LANDSAT pixels, called patches, whose elements are characterized by spectral similarity, within certain tolerances, to their neighbors.

Assumption 1: Real classes exist.

Assumption 2: Each patch contains pixels from one and only one real class.

Assumption 3: Each real class is represented by at least one patch.

No absolute commitment to the agricultural nature of real classes is expressed in [1]; however, there is an indication of a high degree of purity of patches with respect to ground truth labels when AMOEBA patches are plotted on ground truth maps. A more complete study, with the same conclusion, is reported in [5]. Therefore, we feel justified in identifying the real classes with ground truth labels. In addition to the three assumptions just given,

HISSE requires the following assumption.

Assumption 4: The data from each patch is normally distributed with mean and covariance depending only on the class to which it belongs.

Assumption 4 has been challenged, some might say refuted, in [2]. However, we take the position that the proper question to ask is whether assumption 4 is close enough to the truth to be useful in estimating class proportions and labeling classes with ground truth labels. The clustering portion of AMOEBA may be described as a k-means algorithm which respects patch integrity (see Assumption 2) with a novel way of determining the correct number of clusters. As such, it contains no way of compensating for the confusion arising from classes with overlapping spectral characteristics. Thus, Assumption 4 may be regarded as a step toward mitigating the error in proportion estimation which is unavoidable with the classify and count method. Henceforth, pixels contained in patches will be called pure pixels, and all others boundary pixels.

## 2. Mathematical Description.

It is assumed that there are  $m$  real classes, labelled  $1, \dots, m$ , and  $p$  patches represented by independent random vectors  $(X_1, \theta_1), \dots, (X_p, \theta_p)$  where  $\theta_j \in \{1, \dots, m\}$  is the unknown real class to which patch  $j$  belongs and  $X_j = (X_{j1}, \dots, X_{jN_j})$  is a set of  $N_j$   $n$ -vectors representing the spectral data from the  $j$ th patch. The  $\theta_j$  are i.i.d. with  $\alpha_\ell = \text{Prob}[\theta_j = \ell]$  unknown and, given that  $\theta_j = \ell$ ,  $X_j$  is a random sample from an  $n$ -variate normal distribution  $N_n(\mu_\ell, \Omega_\ell)$  with unknown mean and covariance. Notice that  $\alpha_\ell$  is the expected

fraction of patches belonging to class  $\ell$  and for a given scene may be quite different from the fraction of pure pixels belonging to class  $\ell$ , which we denote by  $\phi_\ell$ . The random variable  $\phi_\ell$  is directly related to the total acreage of the patches belonging to class  $\ell$ .

The log likelihood function for the parameters  $\alpha_\ell, \mu_\ell, \Omega_\ell$  is

$$1) \quad L = \sum_{j=1}^p \log f(X_j)$$

where

$$2) \quad f(X_j) = \sum_{\ell=1}^m \alpha_\ell f_\ell(X_j)$$

and  $f_\ell(X_j)$  is the  $N_j$ -fold product normal density

$$3) \quad f_\ell(X_j) = \prod_{k=1}^{N_j} N_n(X_{jk}; \mu_\ell, \Omega_\ell).$$

Despite the apparent complexity of  $L$ , it depends on the data only through the patch means

$$4) \quad m_j = \frac{1}{N_j} \sum_{k=1}^{N_j} X_{jk}$$

and scatter matrices

$$5) \quad S_j = \sum_{k=1}^{N_j} (X_{jk} - m_j)(X_{jk} - m_j)^T$$

Once the  $m_j$ 's and  $S_j$ 's are computed and stored, HISSE has no further need for the pure data.

The numerical procedure used in HISSE for finding a maximum of the likelihood function is defined by iteratively substituting into the likelihood equations, viz.

$$(6) \quad \alpha_{\ell}^{(k+1)} = \frac{1}{p} \sum_{j=1}^p \frac{\alpha_{\ell}^{(k)} f_{\ell}(X_j)}{f(X_j)}$$

$$(7) \quad \mu_{\ell}^{(k+1)} = \frac{p}{\sum_{j=1}^p N_j} \frac{f_{\ell}(X_j)}{f(X_j)} m_j / \sum_{j=1}^p N_j \frac{f_{\ell}(X_j)}{f(X_j)}$$

$$(8) \quad \Omega_{\ell}^{(k+1)} = \frac{p}{\sum_{j=1}^p} \frac{f_{\ell}(X_j)}{f(X_j)} R_j / \sum_{j=1}^p N_j \frac{f_{\ell}(X_j)}{f(X_j)} - \mu_{\ell}^{(k+1)} \mu_{\ell}^{(k+1)T},$$

where  $R_j = S_j + N_j m_j m_j^T$  is the noncentral scatter of the  $j$ th patch. The values of the parameters used in evaluating the ratios  $\frac{f_{\ell}(X_j)}{f(X_j)}$  are those at the preceding  $k$ th step of the algorithm. It is shown in [6] that there is a unique strongly consistent solution of the likelihood equations in a neighborhood of the true parameters as  $p \rightarrow \infty$  and that the iteration procedure (6)-(8) converges to the consistent solution if the starting values are near it.

Let  $N = N_1 + \dots + N_p$  be the total number of pure pixels. It is easy to show that  $E[\phi_{\ell}] = \alpha_{\ell}$  and  $\text{var}(\phi_{\ell}) \leq \frac{1}{4N^2} \sum_{j=1}^p N_j^2$ . Thus, if the patches are nearly uniform in size, the MLE of  $\alpha_{\ell}$  can be used as a predictor of  $\phi_{\ell}$ . However, the least MSE predictor of  $\phi_{\ell}$  based on the observed data (assuming that the parameters are known) is

$$9) \quad \beta_{\ell} = E[\phi_{\ell} | X_1, \dots, X_p] = \frac{1}{N} \sum_{j=1}^p N_j \frac{\alpha_{\ell} f_{\ell}(X_j)}{f(X_j)}.$$

Therefore, we take  $\beta_\ell$  evaluated with the maximum likelihood estimates of the parameters as our estimate of  $\phi_\ell$ .

In processing the boundary pixels, which typically constitute 60-70% of the scene, we assume that the boundary data consist of an independent sample from a mixture

$$10) \quad \sum_{\ell=1}^m \bar{\alpha}_\ell N_n(\mu_\ell, \Omega_\ell)$$

where the component normal distributions are the same class distributions represented in the pure data, plus observations from a contaminant class (possibly corresponding to the "not in field" ground truth label) in the tails of the  $N_n(\mu_\ell, \Omega_\ell)$ . In other words, we assume that a boundary observation which is spectrally unlike all of the pure classes is much more likely to be from the contaminating class than an outlier from one of the pure classes. Therefore we classify as a contaminant each boundary observation  $X$  which satisfies

$$11) \quad (x - \mu_\ell)^T \Omega_\ell^{-1} (x - \mu_\ell) > \chi_\alpha^2$$

for all  $\ell = 1, \dots, m$ , where the  $\mu_\ell$ 's and  $\Omega_\ell$ 's are the previously estimated pure data class means and covariances and  $\chi_\alpha^2$  is a size  $\alpha$  critical value for  $\chi^2$  with  $n$  degrees of freedom. In this experiment we chose  $\alpha = .1$ .

Let  $Y_1, \dots, Y_M$  denote the boundary observations remaining after rejecting those classified as contaminants. We treat  $Y_1, \dots, Y_M$  as an independent sample from the mixture density (10), with unknown mixing proportions  $\bar{\alpha}_1, \dots, \bar{\alpha}_m$



but known components  $N_n(\mu_\ell, \Omega_\ell)$ , and obtain a MLE of  $\bar{\alpha}_1, \dots, \bar{\alpha}_m$  by successively substituting into (6). Obviously,  $Y_1, \dots, Y_M$  is, at best, a truncated sample from the mixture (10), so that the MLE of  $\bar{\alpha}_1, \dots, \bar{\alpha}_m$  is asymptotically biased. We do not expect this effect to be a reason for serious concern. After obtaining the MLE for  $\bar{\alpha}_1, \dots, \bar{\alpha}_m$ , we use as our final estimate of the number of pixels corresponding to class  $\ell$ , the quantity  $N\beta_\ell + M\bar{\alpha}_\ell$ , where  $\beta_\ell$  is given by (9).

### 3. Implementation.

The number of classes assumed in this experiment is determined by AMOEBA subroutines PAINT and CLASFY. PAINT produces the pure/boundary division of a  $5 \times 6$  mile LACIE segment, an array LABELS containing a patch description for each of the pure pixel locations, and a map of the scene showing the pure and boundary pixels. CLASFY produces an array CLASS containing the final cluster designation of each of the patches. A subroutine STAT2 has been attached to AMOEBA which calculates and saves patch sizes  $(N_j)$ , patch means  $(m_j)$  and noncentral patch scatters  $(R_j)$ . These statistics are then passed to STAT3 which uses the CLASS array to compute the fraction  $(\alpha_\ell^0)$  of patches assigned to each cluster, the fraction of pure pixels assigned to each cluster, and cluster means  $(\mu_\ell^0)$  and covariances  $(\Omega_\ell^0)$  for the pure data only. These cluster statistics are used as initial estimates of the parameters for the iteration procedure described by (6)-(8). CLASFY occasionally produces a cluster with such a small number of pure pixels that an initial covariance estimate cannot be calculated. In this case the initial  $\Omega_\ell^0$  in HISSE is obtained by averaging the cluster sample covariance with a multiple of the identity so as to insure that the condition number of  $\Omega_\ell^0$  is no greater than 16.

After initialization HISSE produces iterative estimates  $\alpha_\ell^{(k)}, \mu_\ell^{(k)}, \Omega_\ell^{(k)}$  of the parameters until a convergence criterion is satisfied, after which the estimates  $\beta_\ell$  are computed in the manner described in Section 2 and stored.

The boundary pixels are identified from the LABELS array output by AMOEBA. For each one, the quadratic forms  $(x-\mu_\ell)^T \Omega_\ell^{-1} (x-\mu_\ell)$  are computed and tested against the threshold value of  $\chi_\alpha^2$ , as in (11). For those boundary pixels not rejected by the thresholding procedure, the likelihood ratios  $f_\ell(x)/f_k(x)$  are computed and stored in a temporary disc file for use in the iteration procedure for estimating  $\bar{\alpha}_1, \dots, \bar{\alpha}_m$ . Although the number of boundary pixels processed is much greater than the number of patches, the cost is comparable to that of processing the pure data because the iteration procedure (6) can be carried out simply by accessing the temporary file.

For the purpose of labeling classes HISSE identifies for each class  $\ell$ , the three patches  $j$  which have the highest posterior probability  $\frac{\alpha_\ell f_\ell(x_j)}{f(x_j)}$  in that class. The spatial coordinates of pixels in these labeling patches are obtained from the LABELS array. Thus, in using HISSE, the analyst would be required to make a judgement concerning the identity of each class based on his ability to label the labeling patches.

#### 4. Numerical Results.

The results tabulated in this section are from four passes over LACIE segment 1618 acquired in May, June, August and September of 1976. The data was preprocessed by premultiplying each single pass 4-dimensional data vector by the LANDSAT I transformation to brightness-greenness space

$$\begin{pmatrix} 1 & 1 & 1 & 0 \\ 0 & -1 & 1 & 1 \end{pmatrix}$$

and stacking the brightness-greenness vectors to obtain 8-dimensional data vectors. The results of the AMOEBA run were 7500 pure pixels, organized into 310 patches. The number of clusters estimated by NUMCLU was 13. HISSE required 19 iterations to estimate the parameters of the pure data mixture model. Of the 15290 boundary pixels, the thresholding procedure rejected 5575. The number of passes through the remaining 9725 boundary pixels required to produce estimates of the boundary mixing proportions  $\bar{\alpha}_1, \dots, \bar{\alpha}_{13}$  was 8. The total cost of running AMOEBA and HISSE together is much less than that of running UHMLE or CLASSY on the full scene.

Figures 1-4 show the scatter plots in brightness-greenness space, corresponding to each of the passes, of the means of the patches determined by AMOEBA. Particularly in the fourth pass, the tasseled cap configuration described in [4] is visible. Figures 5, 6, and 7 show the plotted trajectories of the estimated class means from pass to pass on the same coordinate system used in the 4th pass scatter plot. The trajectories of the means of the pure data clusters produced by AMOEBA would be nearly indistinguishable. It is interesting that the class means trajectories eventually given a small grains label exhibit a characteristic triangular shape. Obviously, this characteristic can be used as an aid in labeling the classes (see [3], for a discussion of this idea).

Figure 8 tabulates the initial cluster means, cluster variances, and patch membership proportions obtained from AMOEBA's clustering of the pure data. Figure 9 tabulates class means, variances and patch membership probabilities (the  $\alpha$ 's) estimated by HISSE. Figure 10 compares the estimates derived from AMOEBA and HISSE of the fraction of pure pixels belonging to each cluster (class). Notice that in Figure 10, there is a significant difference between the two estimates, particularly in the more populous classes. These classes happen to be the most

spectrally confused classes. There is also an appreciable difference seen in Figures 8 and 9 between the respective estimates of the  $\alpha$ 's, although the difference is not as pronounced.

Figure 11 shows the AMOEBA boundary map for segment 1618 with the three labeling patches corresponding to each class outlined. A ground truth map was used to attach ground truth labels to the labeling patches and hence to the classes. Most of the classes were given a single ground truth label by this procedure. Classes 2, 5, 6, 7, were not assigned a single ground truth label and appeared to be made up of more than one type of small grains. However, each of these classes was clearly small grains. Class 1 was the only really difficult class to label; each of its labeling patches represented small grains ground truth labels as well as such labels as beans and fallow. In other words, the labeling patches for class 1 were spurious. For the purpose of obtaining an aggregate small grains estimate, it was assumed that class 1 was a mixture of 1/3 small grains, 1/3 beans, and 1/3 fallow acreage.

Figure 12 shows the final acreage estimate for each of the 13 classes in the mixture model, the acreage of the set C of boundary pixels rejected as outliers or contaminants, and the crop labels (including "small grains") assigned to each class. The aggregate small grains acreage estimate is 15,288. The small grains acreage from the ground truth tape is 15,465, an error of only 1.1%. If class 1 is labelled all small grains, the error is 15%. If none of class 1 is classified small grains, the error is 9.2%. It should be emphasized that the problem of labeling cluster #1 from AMOEBA is also serious, since cluster 1 is centered near the means of the spurious patches used to label class 1.

The thresholding of boundary outliers makes a pronounced difference in the

estimate. The small grains acreage estimate derived from HISSE without thresholding would be 19,230, comparable to the estimate of 20,336 derived from AMOEBA's cluster map.

## 5. Conclusions.

The accuracy with which HISSE estimated the small grains acreage in segment 1618 was impressive, to say the least, but of course the procedure must be tested on other segments for which ground truth is available. Also, as we mentioned in Section 4, the accuracy of the estimate depends on the classification given to the labeling fields for class 1, the problem class. The procedure we used - dividing the class evenly among competing ground truth labels - seems fair; however, in an operational situation the class would be labeled by an analyst looking at a film product and it seems unlikely that he would apportion the class in such a way. In any case, the greatest possible relative error was 15%, still a marked improvement over the accuracy obtained by labeling AMOEBA's clusters and counting the cluster assignments, or that achieved by HISSE without the thresholding procedure.

The performance of HISSE, or AMOEBA, depends in large part upon the purity with respect to ground truth labels of the patches found by AMOEBA, which is influenced by the user defined "percent in fields" parameter in AMOEBA. In this experiment we defined the parameter as 50%; that is, we conservatively estimate that 50% of the pixels in the scene should be found in fields. By reducing the size of this parameter, we expect to produce a higher degree of patch purity and thus alleviate the problem of having a class represented by labeling patches which should not be patches at all. We hope that this will not aggravate another

problem, namely that the ground truth map for segment 1618 shows a few large fields representing important classes (such as barley) in which no patches were found.

Finally, we note that although the aggregated small grains acreage was very accurately estimated, the individual estimates for the various small grains classes (spring wheat, barley, oats, and millet) were not nearly as accurate. Indeed, several of the HISSE classes could not be given a single one of these labels, although they clearly represented small grains. Moreover, there was one significant crop class (beans) without a small grains label which was seriously underestimated. Thus, the usefulness of HISSE in a multicrop inventory cannot yet be determined.

## REFERENCES

1. Jack Bryant, On the clustering of multidimensional pictorial data, Pattern Recognition, 11(2), pp. 115-125, 1979.
2. W. D. Davenport and S. G. Wheeler, Multispectral data analysis based on ground truth crop classes. IBM Report No. RES 23-83, IBM Federal Systems Division, Houston, Texas, May 1980.
3. J. L. Engvall, D. Tubbs, and Q. A. Holmes, Pattern recognition of Landsat data based upon temporal trend analysis. Remote Sensing of the Environment, 6, 303-314, (1977).
4. R. J. Kauth and G. Thomas, The tasseled cap—a graphic description of the spectral-temporal development of agricultural crops as seen by Landsat, Purdue/LARS Symposium on Machine Processing of Remotely Sensed Data, Purdue University, 1976.
5. R. M. Myers, Spatial-spectral procedure development: the purity experiment, IBM Report No. SR-10-00445, IBM Federal Systems Division, Houston, Texas, April 1980.
6. B. C. Peters, Jr., On the consistency of the maximum likelihood estimate of normal mixture parameters for a sample with field structure. Report No. 74, Department of Mathematics, University of Houston, Sept. 1979.

FILE NUMBER (CONTINUATION DATE = 06-15-00)  
 SCATTERGRAM OF (PASS) Y

1618  
 PASS 1

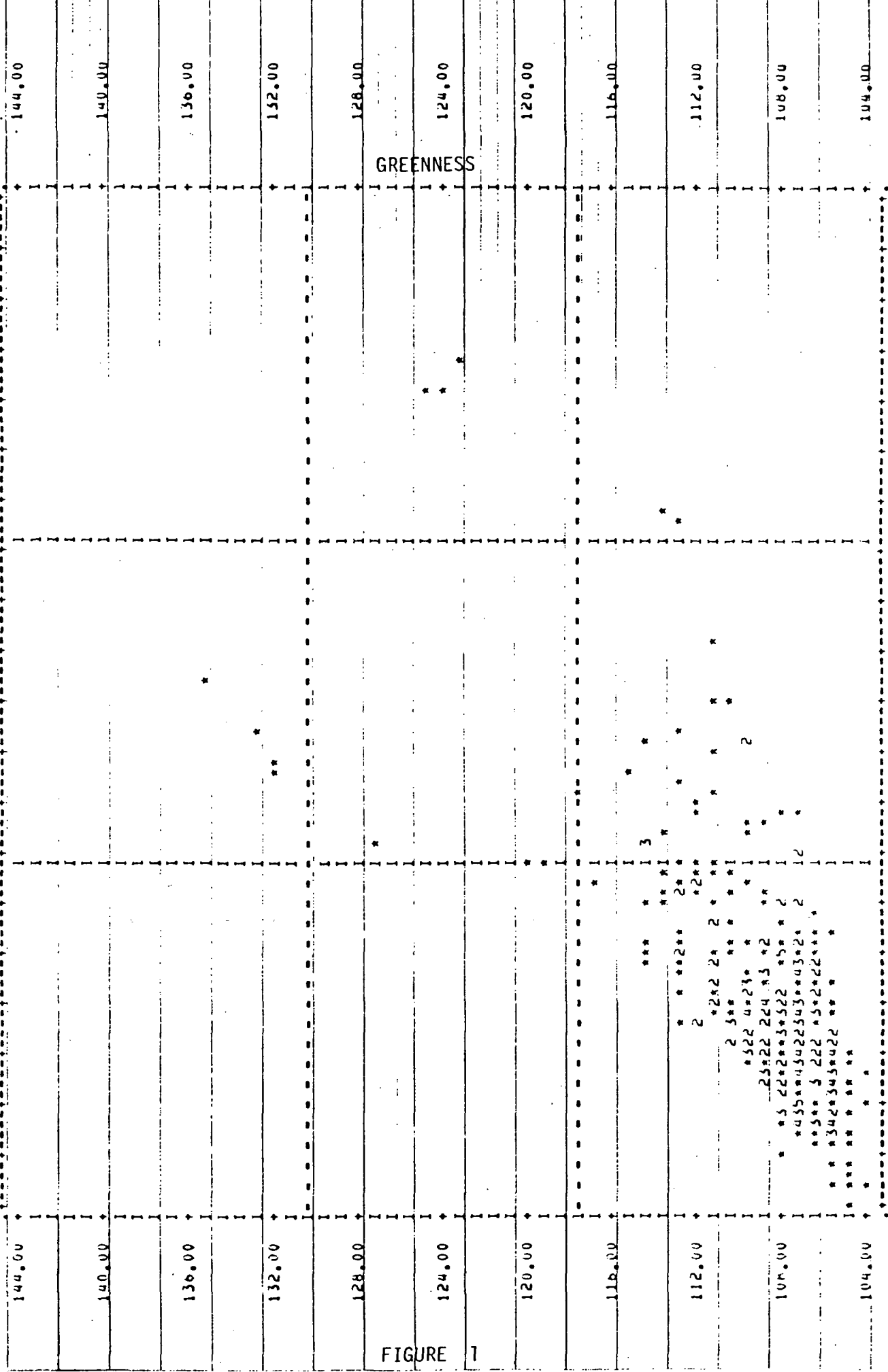


FIGURE 1

BRIGHTNESS



FILE NUMBER (CREATION DATE = 08-15-80)  
SCATTERGRAM OF (COUNT) Y  
25,00 27,00 29,00 31,00 33,00 35,00 37,00 39,00 41,00

Wavelength (nm)	Intensity (Counts)	Wavelength (nm)	Intensity (Counts)
145.00	145.00	25.00	25.00
141.00	141.00	27.00	27.00
137.00	137.00	29.00	29.00
133.00	133.00	31.00	31.00
129.00	129.00	33.00	33.00
125.00	125.00	35.00	35.00
121.00	121.00	37.00	37.00
117.00	117.00	39.00	39.00
113.00	113.00	41.00	41.00
109.00	109.00		
105.00	105.00		

GREENNESS

FIGURE 2

BRIGHTNESS

1618  
PASS 3

FILE 00527 (CALIBRATION DATE = 05-15-60)  
SCATTERGRAM OF (GROSS) Y

143.00	139.00	135.00	131.00	127.00	123.00	119.00	115.00	111.00	107.00	103.00
20.00	20.00	20.00	20.00	20.00	20.00	20.00	20.00	20.00	20.00	20.00
32.00	32.00	32.00	32.00	32.00	32.00	32.00	32.00	32.00	32.00	32.00
40.00	40.00	40.00	40.00	40.00	40.00	40.00	40.00	40.00	40.00	40.00
46.00	46.00	46.00	46.00	46.00	46.00	46.00	46.00	46.00	46.00	46.00
50.00	50.00	50.00	50.00	50.00	50.00	50.00	50.00	50.00	50.00	50.00
52.00	52.00	52.00	52.00	52.00	52.00	52.00	52.00	52.00	52.00	52.00
54.00	54.00	54.00	54.00	54.00	54.00	54.00	54.00	54.00	54.00	54.00
56.00	56.00	56.00	56.00	56.00	56.00	56.00	56.00	56.00	56.00	56.00
58.00	58.00	58.00	58.00	58.00	58.00	58.00	58.00	58.00	58.00	58.00
62.00	62.00	62.00	62.00	62.00	62.00	62.00	62.00	62.00	62.00	62.00

FIGURE 3

GREENNESS

BRIGHTNESS

1618  
PASS 4

FILE NAME (CROSS) A  
SCATTERING OF (000) Y

15.00	19.00	23.00	27.00	31.00	35.00	39.00	43.00	47.00	51.00
141.00									
137.00									
133.00									
129.00									
125.00									
121.00									
117.00									
113.00									
109.00									
105.00									
101.00									

GREENNESS

FIGURE 4

BRIGHTNESS

FINAL CLASS TRAJECTORIES

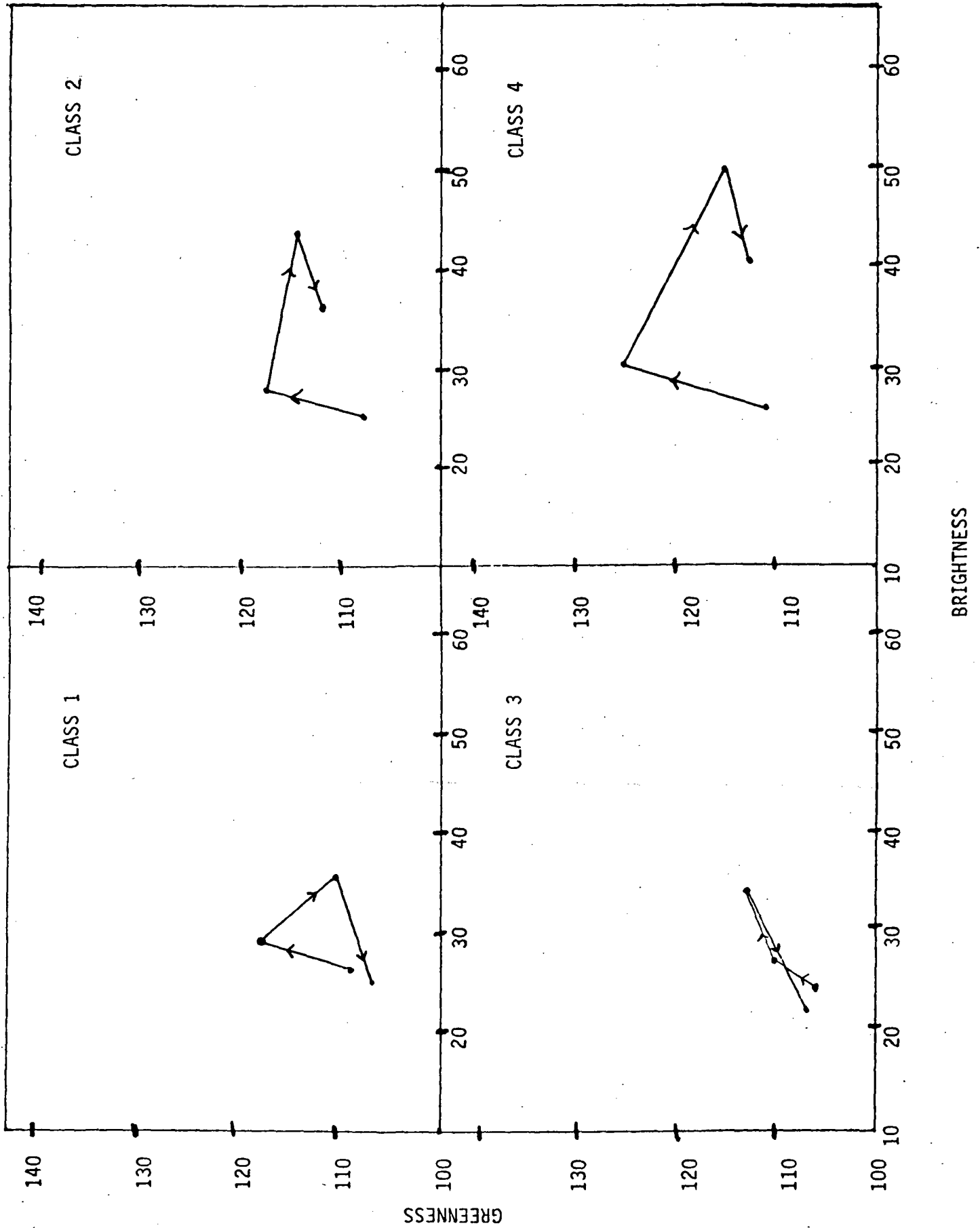


FIGURE 5

# FINAL CLASS TRAJECTORIES

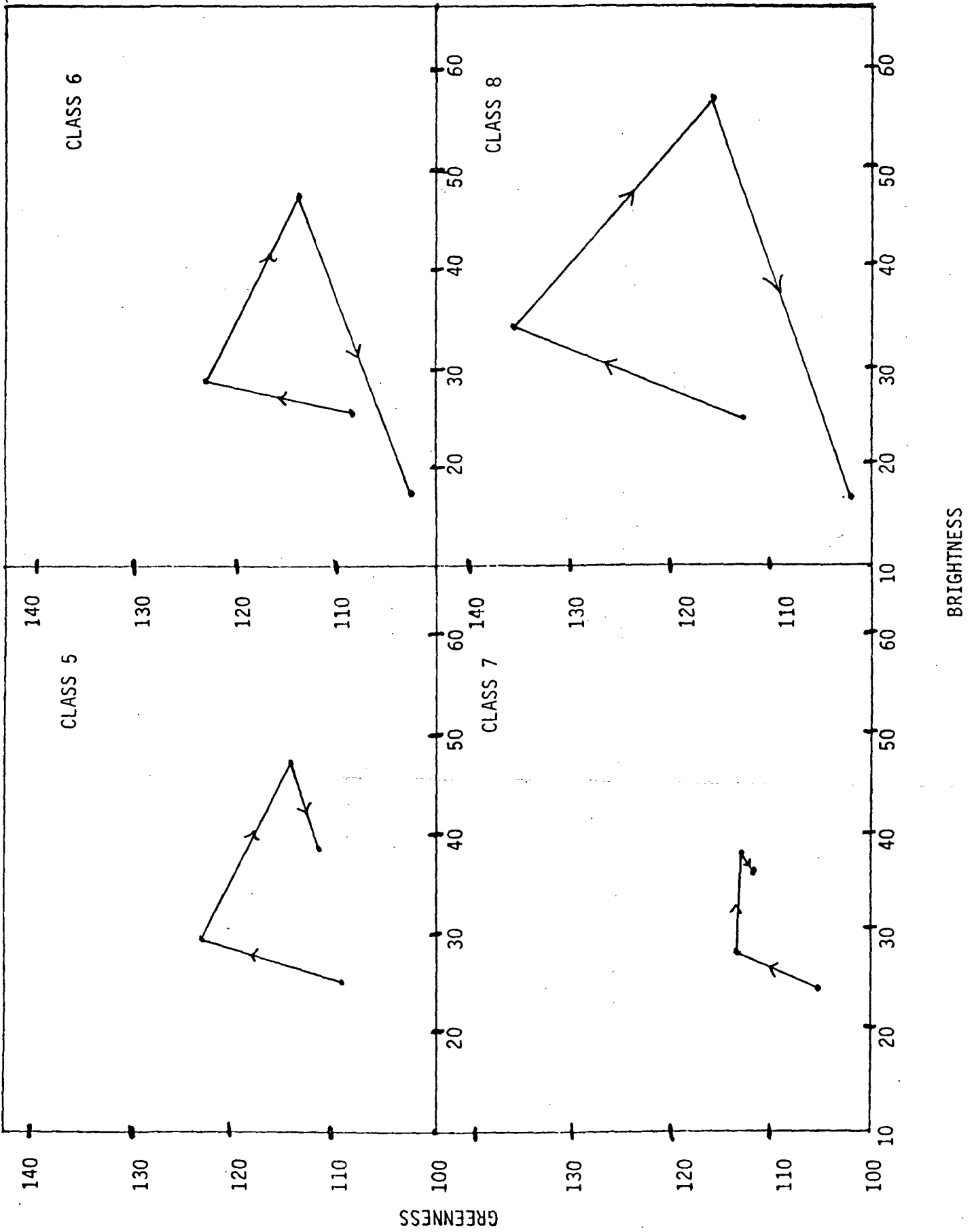


FIGURE 6

# FINAL CLASS TRAJECTORIES

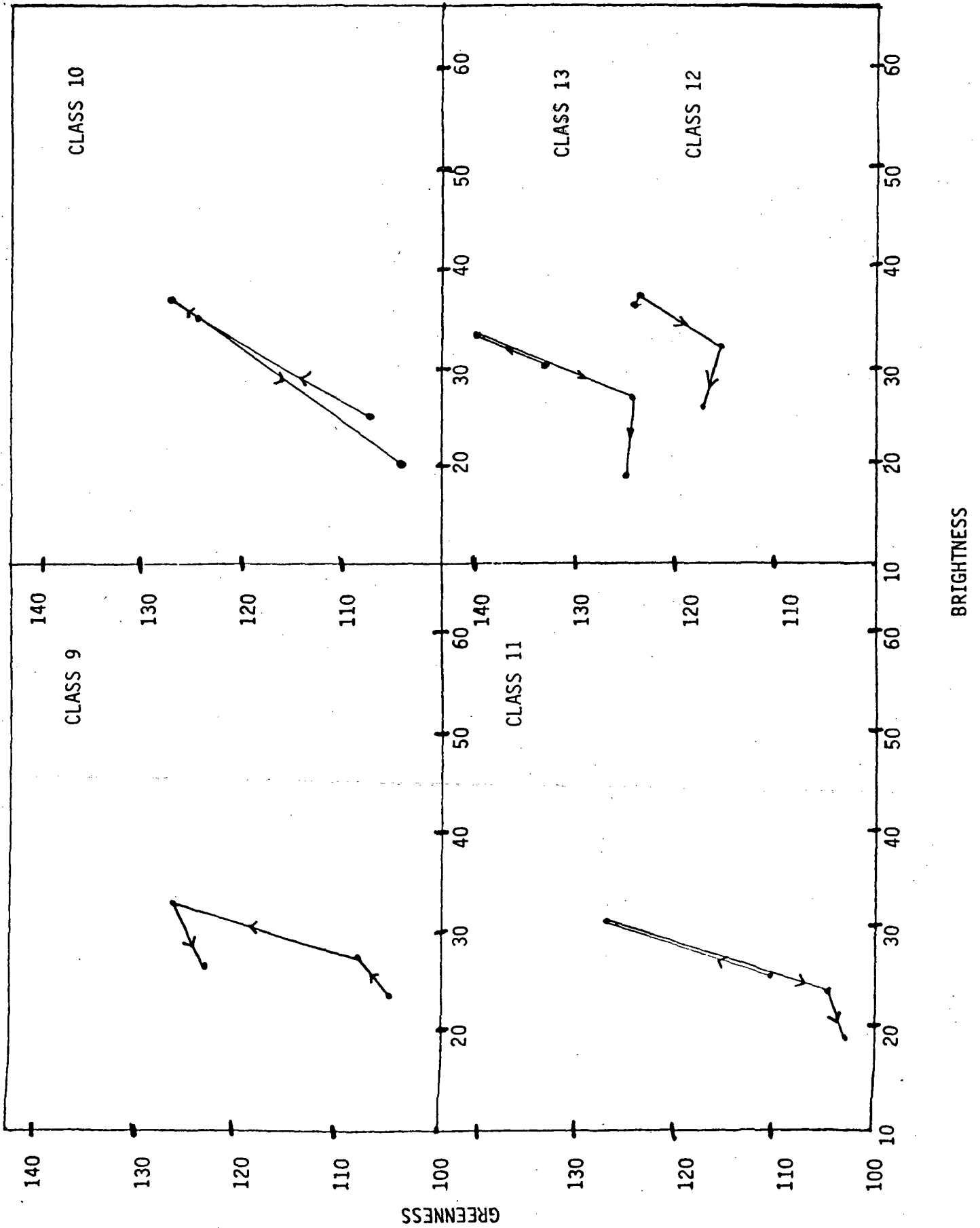


FIGURE 7

CLUSTER #	CLUSTER MEAN									PATCH PROPORTION
1	26.84	110.39	29.79	121.70	36.49	111.02	26.44	108.04		.077
2	24.99	108.48	28.17	117.42	44.25	115.57	34.05	112.63		.094
3	24.80	106.86	28.82	111.90	32.59	111.73	21.69	107.00		.271
4	25.51	111.64	30.29	127.63	50.08	115.15	39.10	113.13		.094
5	25.46	108.75	29.26	122.53	48.90	114.94	36.61	111.77		.100
6	25.09	109.24	29.35	123.39	48.80	114.94	18.15	103.83		.158
7	23.90	106.14	28.76	113.53	38.15	113.07	37.15	112.73		.058
8	25.05	112.20	33.45	135.38	56.52	116.32	17.19	102.97		.026
9	23.26	105.98	29.02	108.48	34.30	125.54	25.91	121.94		.048
10	25.50	107.50	35.75	123.25	37.25	126.50	20.25	104.75		.003
11	25.49	110.83	30.71	128.90	24.92	104.16	19.04	104.01		.045
12	37.60	123.64	37.76	123.44	31.92	116.60	25.48	118.12		.010
13	30.16	132.47	31.80	139.64	27.37	123.07	20.68	123.83		.016

## CLUSTER VARIANCE

1	7.98	10.82	3.22	36.25	51.31	16.82	32.68	10.60
2	6.09	10.51	3.25	25.33	33.50	8.50	23.18	18.36
3	7.87	5.24	7.29	32.49	29.88	18.48	17.25	12.48
4	4.54	18.49	2.48	15.77	32.80	7.96	16.41	5.97
5	9.11	4.70	3.13	21.46	27.59	6.43	19.92	6.90
6	4.64	8.34	4.26	38.13	44.59	6.00	11.12	6.22
7	4.74	2.60	6.14	22.52	15.73	11.22	37.19	7.90
8	1.50	3.18	3.61	12.71	15.00	1.84	3.43	1.59
9	2.90	3.42	5.40	11.30	11.44	24.02	8.12	53.75
10	4.25	0.25	0.69	35.19	11.19	4.25	1.19	3.69
11	4.00	5.83	5.35	33.79	5.26	1.55	8.07	3.38
12	3.28	2.56	2.90	3.69	1.43	3.61	3.93	3.95
13	1.75	9.97	1.38	5.20	1.31	2.81	1.09	3.41

FIGURE 8

FINAL CLASS STATISTICS (HISSE)

CLASS #	CLASS MEAN									PATCH PROBABILITY
1	26.91	109.19	29.64	117.57	35.07	110.50	25.53	107.45		.126
2	24.62	108.52	27.91	117.84	44.68	115.93	35.13	113.58		.083
3	24.11	106.34	28.61	110.87	33.73	113.30	21.65	107.51		.221
4	25.58	111.88	30.23	126.89	50.83	115.51	39.97	113.64		.084
5	25.30	108.73	29.41	123.19	48.09	114.35	35.83	111.28		.108
6	25.10	109.25	29.36	123.38	48.73	114.95	18.20	103.89		.170
7	23.89	106.13	28.78	113.49	38.08	113.06	37.04	112.70		.061
8	25.06	112.25	33.47	135.41	56.65	116.35	17.13	102.93		.023
9	23.26	105.98	29.02	108.48	34.30	125.55	25.91	121.94		.048
10	25.50	107.50	35.75	123.25	37.25	126.50	20.25	104.75		.003
11	25.25	110.37	29.80	127.20	24.86	104.14	19.07	103.99		.048
12	37.60	123.64	37.76	123.44	31.92	116.60	25.48	118.12		.010
13	30.16	132.47	31.80	139.64	27.37	123.07	20.68	123.83		.016

CLASS VARIANCE

1	9.56	10.44	5.08	51.15	72.18	24.81	44.57	12.14
2	3.76	10.02	2.71	23.47	35.32	8.02	15.39	17.05
3	4.66	3.29	6.93	25.02	21.94	9.55	14.74	13.05
4	4.78	20.68	2.74	19.15	39.22	7.15	16.30	4.31
5	9.48	4.02	2.98	26.54	20.81	4.94	18.06	6.76
6	4.60	8.04	4.29	38.42	44.64	5.61	11.24	6.09
7	4.66	2.34	6.15	22.65	15.92	11.02	37.65	7.82
8	1.53	3.19	3.62	12.65	14.57	1.81	3.33	1.50
9	2.89	3.24	5.36	11.27	11.47	23.77	8.18	53.66
10	4.25	0.26	0.69	35.20	11.19	4.25	1.19	3.70
11	3.78	5.89	8.48	42.06	4.79	1.75	6.84	2.88
12	3.07	3.24	3.00	3.00	1.31	3.32	4.07	3.66
13	1.64	9.20	1.49	5.16	1.30	2.49	0.99	3.85

FIGURE 9



PURE PIXEL PROPORTIONS( $\phi_k$ )

CLUSTER #	AMOEBE ESTIMATE	CLASS #	HISSE ESTIMATE( $\beta_k$ )
1	.054	1	.143
2	.136	2	.107
3	.259	3	.188
4	.101	4	.089
5	.109	5	.123
6	.171	6	.174
7	.067	7	.068
8	.021	8	.021
9	.034	9	.034
10	.001	10	.001
11	.031	11	.038
12	.003	12	.003
13	.012	13	.012

FIGURE 10





### CLASS ACREAGE ESTIMATES

CLASS	ACREAGE	CROP LABEL
1	3764	Small Grains Beans Idle Fallow
2	1550	Small Grains
3	3560	Spring Wheat
4	1237	Spring Wheat
5	2253	Small Grains
6	3257	Small Grains
7	1218	Small Grains
8	262	Spring Wheat
9	917	Idle Cover Crop
10	4	Flax
11	697	Barley
12	49	Homestead
13	171	Trees
C	6124	Contaminated Data

FIGURE 12